The Abdus Salam
International Centre for Theoretical Physics

United Nations
Educational, Scientific and
Cultural Organization

IAEA
International Atomic Energy Agency

1965-36

9th Workshop on Three-Dimensional Modelling of Seismic Waves Generation, Propagation and their Inversion

22 September - 4 October, 2008

Tomography and Active Tectonics in Kanto, Japan

Francis T. Wu
Department of Geological Science
State University of New York
Binghamton
New York
USA

francis@binghamton.edu

Tomography and Active Tectonics in Kanto, Japan

Francis T Wu
Department of Geological Science
State University of New York
Binghamton, New York

My recent research interest has been the use of tomography (using earthquakes or combining earthquqakes and active source data) to study mountain ranges. Such study may also benefit from the addition of other data, such as seismicity, GPS, magnetotellurics, active source profiles – in other words, anything that can help.

I will illustrate my experience with two examples. One is a recent study on Japan where good local earthquake data exist. The other is a comprehensive field study of Taiwan that has gone on for four years and a lot of data have come online and papers written but a fairly complex marine and land experiment will take place in spring and early summer.

The Japan study has already been published (pdf included). I will use it to illustrate that unanswered tectonic questions are still aplenty in spite of the intense seismological research effort there. *Please consult this paper for references on the following discussions on Japan*. In these notes I use larger figures with some addition materials.

In a separate set of notes I will discuss my current project in Taiwan. The Taiwan experiment was built from ground up and the planning of it started in Trieste in 2000, shortly after a major earthquake occurred in Taiwan. The TAIGER (TAiwan Integrated GEodynamics Research) is an US-funded program with major funding to participating Taiwan groups.

The interacting of the Philippine Sea and Pacific plates under Kanto

Kanto Plain sits near the region in Japan under which the two plates, the Philippine Sea and the Pacific, subduct under the Eurasian plate, essentially. While the Pacific plate (PAC) subducts toward the west the Philippine Sea plate (PHS) subducts toward the north over it. The 1923 Great Tokyo Earthquake is known to have caused by a fault which is a part of the interface between PHS and the Eurasian plates (EUR).

In addition to the type of earthquakes just mentioned there are evidently other deeper earthquakes under Tokyo that has produced much damages through the Japanese history. In 2004 or so I became intrigued by the question of what happens when PHS and PAC meets at depth? Could they be responsible for the deeper earthquakes? Since the Kobe earthquake in 1995 the seismic network stations were expanded; the network is designed well and the NIED (National Research Institute for Earth Science and Disaster Prevension) arrival database is of high quality. In cooperation with Japanese colleagues Drs. N. Hirata and H. Sato and an US colleague D. Okaya of USC we analyzed the data in some detail.

Figure 1, center around Kanto, shows the topography, seismicity and other features in the area. Also shown are the profile lines for tomography. Although similar

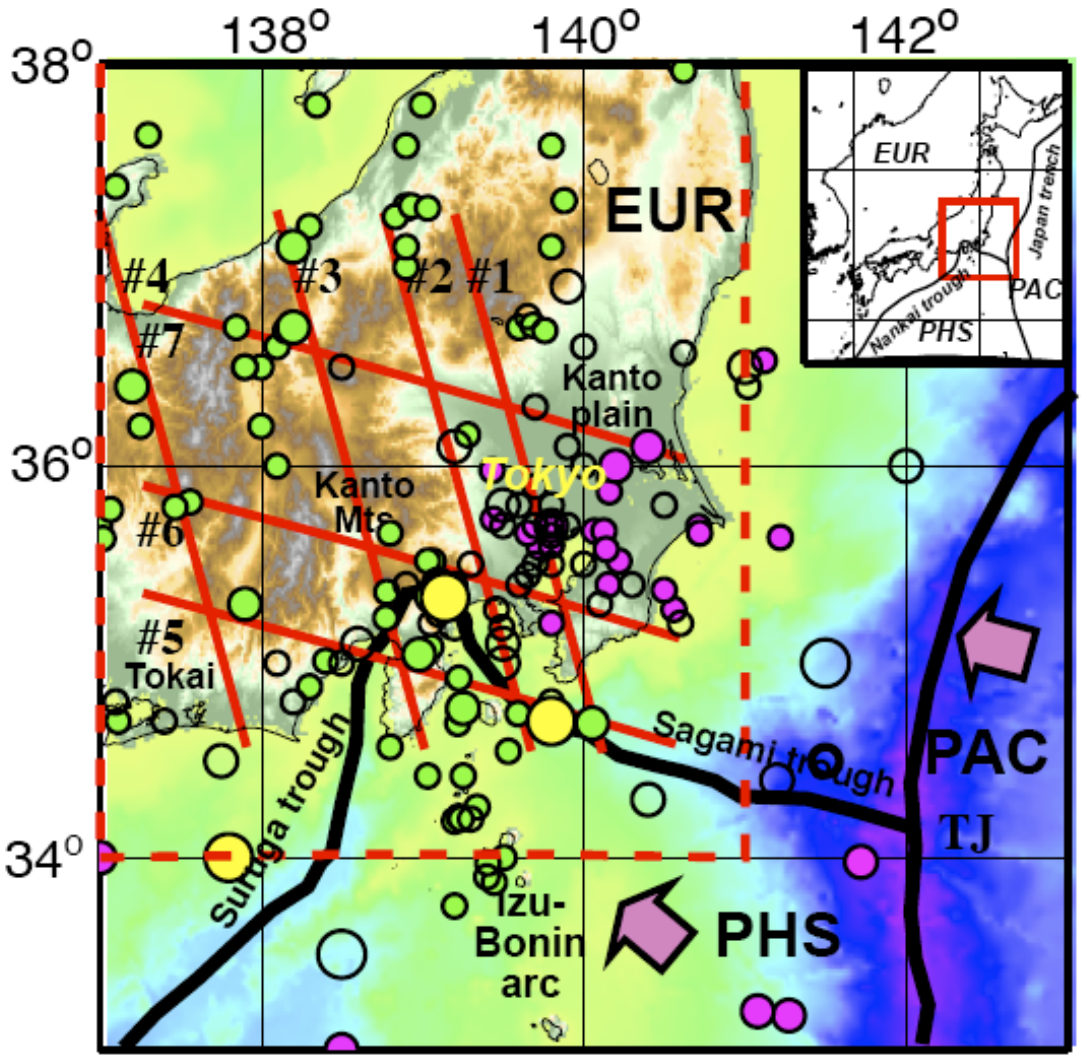

Figure 1. Plate configuration and historical seismicity in Kanto region of central Japan. Philippine Sea (PHS) and Pacific (PAC) plates subduct under Eurasia (EUR) at 4.5 and 10.3 cm/yr, respectively, in directions indicated by arrows. TJ indicates location of EUR-HSPAC triple junction. Damaging historical seismicity during 1600-2006 shown as circles. Circle diameters indicate earthquake magnitude: large=M8, medium=M7, small=M6. Circle colors indicate type of earthquake; yellow=megathrust, green=crustal, magenta=sub-crustal. Open circles denote no depth information or the type was not determined. Red dashed box indicates region of seismic tomography and earthquake relocation analyses. Red solid lines are locations of cross-sections shown in Figure 3. Inset: Location of Figure 1 within central Japan.

figures are shown in the published papers we are adding two more profiles here to enhance what is contained in the paper.

We use a tomographic code written by Benz [1996] in which a 3-D finite difference ray-tracing code is employed. The particular advance of the Benz code is its relatively high resolution and the ability of the ray-tracer to handle rapid velocity changes. We use block size of 5x5x2 km^3. During each iteration both velocity inversion and relocation of sources are carried out.

To make our discussions easier we will present the model we constructed after we study the results of tomography. The conceptual tectonic model in Fig. 2 shows the general plate structures and helps our visualization of the results behind this model. The subregions are: (A) collision between PHS and PAC, (B) simple PHS subduction, (C) collision of Izu-Bonin arc with EUR and ill-defined subduction in Izu and the area to its north, and (D) shallow subduction in the eastern Tokai area. Many of the historical M~6-7 events that caused significant damages in the Kanto area (Fig. 1) are in the structurally shallow portions of Zones A and B.

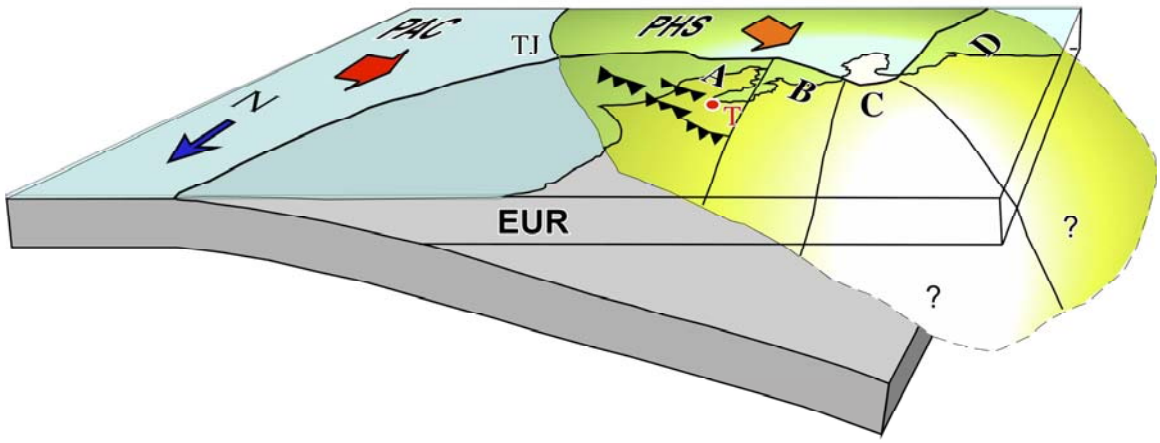

Figure 2. Conceptual model of PHS-PAC-EUR plate configuration. View from northwest. TJ is location of PAC-PHS-EUR triple junction. Red T and dot denote city of Tokyo. A-D are zones of different seismic velocity and seismicity character as defined in text. PHS Zone B toe and Zone A toe and eastern edge interact with PAC. Elevated seismicity and internal deformation exist within Zone A.

The PDF file for the paper by Wu et al. [2007] has most of the details of the basic tectonics of Kanto Plain and the methodology we need here. In Fig. 3 one particular view of the 3-D seismicity is shown. The seismicity associated with different plates are color-coded. There are online materials showing 3-D rotation of the seismicity (relocated, see above) under Kanto. The plate structures can generally be seen from the seismicity. We note that the Wadati-Benioff zone associated with PAC can easily identified by the double-layered seismicity, and the seismicity of PSP is shallower and in zone C it is very

low.

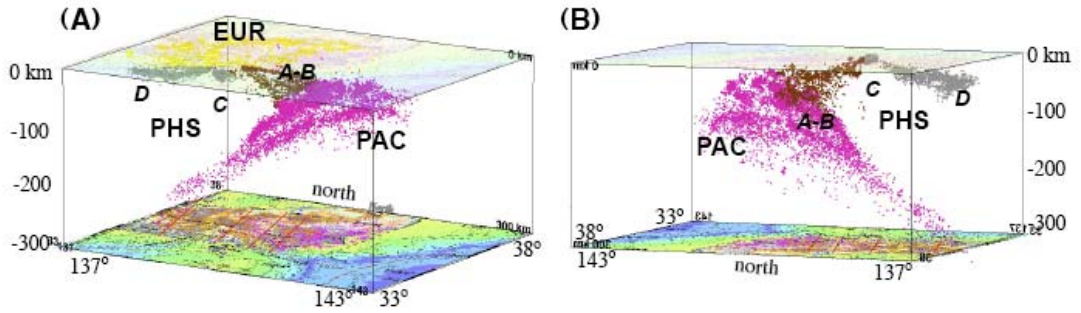

Figure 3. Perspective views of Kanto 3-D seismicity. Views are from (A) south-southeast and (B) north-northwest; full azimuthal coverage available in upplemental Information movie files. EUR and PAC earthquakes in yellow and magenta dots, espectively. PHS earthquakes shown as brown dots for zones A-B and grey dots for Zone D. See text for zones A-D. PAC slab dips towards west and has a well-developed double seismic zone. In View (B) the EUR earthquakes are removed and the view direction looks up the hinge of the PHS arch related to Izu-Bonin arc; the subducted part of this hinge is seismically quiescent (Zone C). Note that eastern Zone A (brown) portion of PHS interacts with PAC.

Tomography

Tomographic sections

Tomographic sections are also plotted both in perturbations from the initial model and the absolute velocity. In Fig. 4a and 4b PAC is easily identified by its double seismic zone in cross- or dip-section (#1-3, #5-7) as well as by its relatively high Vp or positive dVp (#5-7). The arch shape of PAC in (#1-3), both in terms of seismicity and Vp images, is evidently related to the bend in the map trace of the Japan trench near the triple junction (Fig. 1). The arch becomes shallower going from the west (#4) to the east (#1) as the Japan trench is approached. The focal mechanisms for PAC events are dominated by down-dip compression for the top zone and down-dip tension for the bottom zone (Fig. 4). PHS however varies greatly along its strike. In the far west of the study region, west of Izu-Bonin arc, PHS subducts at a shallow angle under Tokai (#4-5). Further to the east in Zone C, along the Izu-Bonin-Kanto Mts. axis, we do not find a clearly defined subduction zone based on Vp, dVp anomalies or seismicity (#3); although at depths below 60 km some high Vp or positive dVp anomalies are observed. In cross-section #5 and #6 the Izu-Bonin arc is seen to overlie the top of an asymmetric high velocity arch that can be seen in #5 and #6. The descending PHS slab is clearly seen in Zone B (#2), with high Vp, positive dVp anomalies and a well-defined Wadati-Benioff zone near the top of the slab; the slab toe is atop of if not touching PAC. For Zone A the enhanced PHS seismicity above PAC, at a depth of ~70 km, is quite visible, not only at the top of the slab but also internal to PHS (#1, #6-7); the high seismicity on top of PAC gives the appearance of PHS-PAC contact.

Although some of the general results we just summarized have been observed in earlier tomographic work, two new features stand out in our imaging. The first one is key to locating the top of the subducting PHS at the crust/upper mantle boundary and the other shows the effects of PHS and PAC interaction. Both of them are distinct from the megathrust mentioned earlier and both may introduce sources of additional seismic hazards. In sections #1 and #2 where the PHS slab enters the mantle, the EUR lower crust is seen to be dragged into the upper mantle (Fig. 4). In Fig. 5 a map view of the 7.5 km/sec iso-velocity surface shows the lateral extent of this drag-down. South of the trough the layer above the 7.5 km/sec surface deepens from 30 km in southern Kanto to about 55 km at its deepest point; to the north of the trough the surface becomes shallow very rapidly. This is direct evidence of crustal materials being dragged down into the mantle during subduction, a process necessary in the creation of ultra-high pressure metamorphic rocks[24]. For our present purpose this drag-down is key evidence to trace the top of PHS as it enters the upper mantle. This east-west oriented feature is limited to the A and B zones and is nearly linear in map view for a distance of more than 150 km across northern Kanto Plain, differing from a curved one as implied by Ishida's[6] contour map of the top of PHS. The drag-down is down-dip from the megathrust, and thrust mechanisms in the zone are common (Fig.4 #1). Our second new feature is the transition from the almost ideal interplate subduction-type seismicity in Zone B (Fig.4 #2) to the intraplate seismicity in Zone A (#1), where multiple layers of seismicity above PAC are found. The focal mechanisms associated with PHS within Zone A (Fig. 4 #1) indicates that the intra-slab deformation is complex and may include slab-breaking back thrusts as well as strike-slip and normal faults.

Matter of resolution

One of the methods tomographers use often to indicate whether there is enough stations and data for tomographically imaging a region is the so-called "checkerboard test". In the test, known anomalies are introduced into the 1-D starting model; using a set of synthetic traveltimes calculated from the same sources and receivers (i.e., earthquakes and stations) one can attempt to recover the anomalies applying the same inversion procedures (but with relocating the events). It is a test to see which parts of the model space can be resolved by the available traveltime dataset. We perform a test with a model including regularly spaced alternatingly positive blocks of 7x7x5 elements, each element being 5x5x2 km in size, with positive and negative 12% anomalies; the velocity anomaly is full 12 % at the center and tapers off to 0 to the edge. In Fig. 6 we show two crosssections co-siting with profiles #2 and #3 in the main paper and in Fig. 7 we show two maps of the recovered anomalies in our study area. In general, under the land areas above 40 kilometers the resolution is good because of the abundant earthquakes above this depth and the large number of recording stations. Even at the depth 96-98 km there is still resolution of the anomalies but the resolvedarea is smaller and their amplitudes smaller. Under Kanto the resolution above PAC is generally good; PAC is however not well resolved because of the dwindling number of events. The checkerboard tests are not of course totally realistic as the ray paths of the waves in the checkerboard model are not the

same as those in the actual Earth. But they do provide guidance in our interpretation. In our interpretation we use seismicity as well to guide us. For example, if the same relation between seismicity and velocity anomalies holds for both well-resolved and ill-resolved areas it is perhaps likely that the results are significant.

Conclusion

From the tomographic sections, together with seismicity and focal mechanisms we this process. The enhanced seismicity in Zone A due to PHS-PAC interaction is extensive. Could these potential source zones produce the historical M6 and M7 events (Fig. 1)? That these structures are potentially seismogenic is demonstrated by the presence of ample seismicity as shown in section #1 of Fig. 4a. To explore the size of the potential fault we consider the dimensions of the structures in question. For example, the top surface of the PHS down-dip from the megathrust has a maximum horizontal length of about 150 km (the length of the pulldown as shown in Fig. 5) and the regions of internal deformation in Zone A have dimensions of ~20 km. Faults with these dimensions are able to generate M6 and M7 events[26]. More focused studies of seismicity and focal mechanisms in the drag-down region and in Zone A are needed in order to determine the possible existence of large rupture surfaces, hidden from direct view at the earth surface but which represent potential rupture sites for upcoming M6 and M7 earthquakes. Future estimations of seismic hazards for urban Tokyo must take into account the PHS intraslab deformation earthquakes due to slab-slab interaction with PAC in addition to the top-of-PHS megathrust earthquakes.

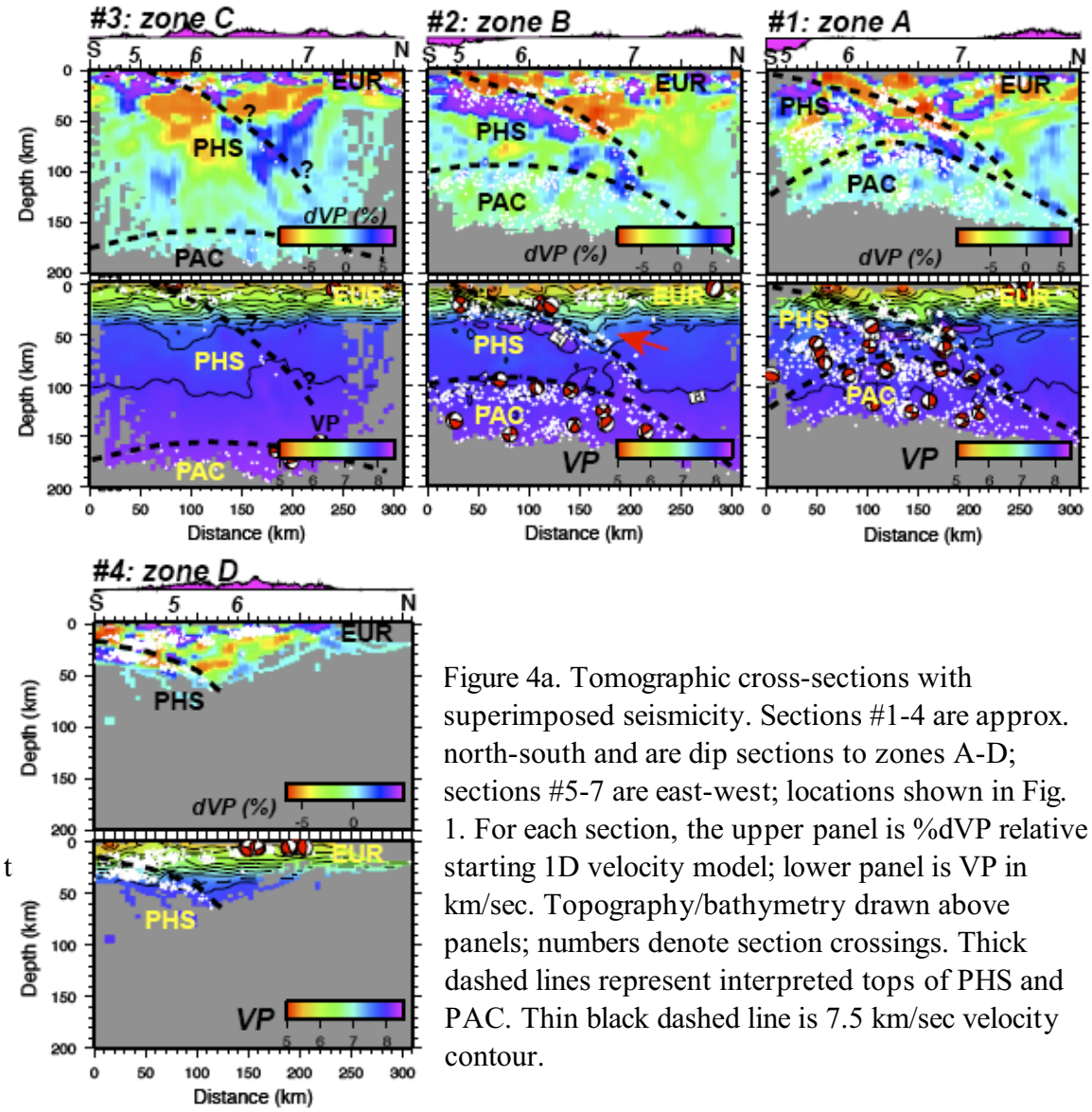

Figure 4a. Tomographic cross-sections with superimposed seismicity. Sections #1-4 are approx. north-south and are dip sections to zones A-D; sections #5-7 are east-west; locations shown in Fig. 1. For each section, the upper panel is %dVP relative starting 1D velocity model; lower panel is VP in km/sec. Topography/bathymetry drawn above panels; numbers denote section crossings. Thick dashed lines represent interpreted tops of PHS and PAC. Thin black dashed line is 7.5 km/sec velocity contour.

t

#1: Zone A: Enhanced PHS seismicity above PAC double seismic zone.
#2: Zone B: Subducting PHS whose toe hits PAC. Note PAC double seismic zone. Tectonic erosion of EUR due to PHS subduction (arrow).
#3: Zone C: Quiescent PHS has uncertain VP expression. PAC just visible at depth.
#4: Zone D: Tokai subduction of PHS.

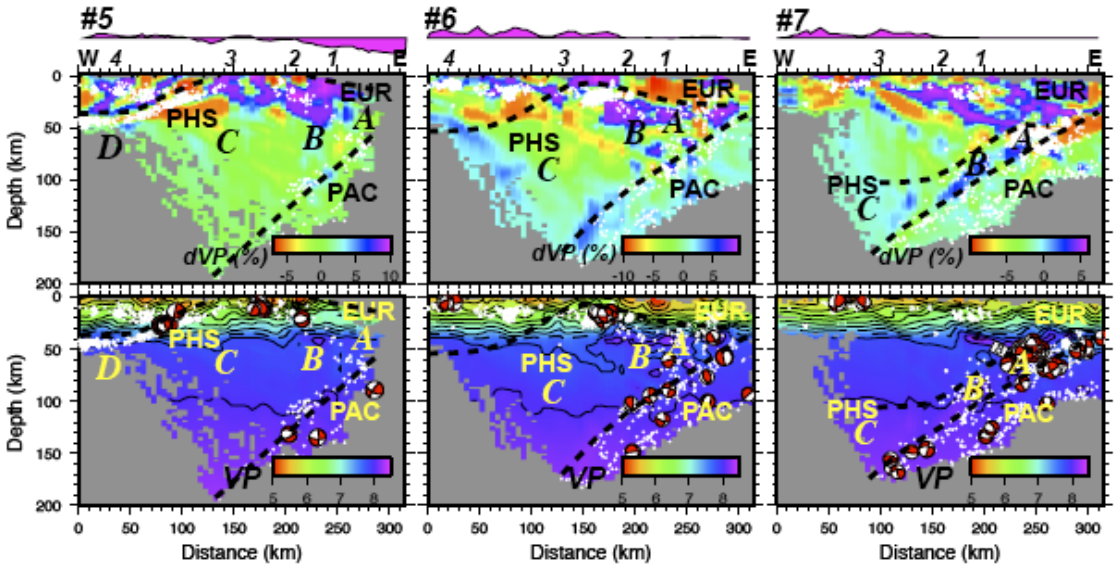

Figure 4b. (See Figure 4a caption.)
#5: Arched PHS interacting with PAC. Subsurface locations of zones A-D labeled.
#6: Quiescent PHS (zone C) becomes seismogenic (B), interacts with PAC (A).
#7: Western quiescent PHS (C); eastern PHS toe (B) and edge (A) interacts with subducting PAC.

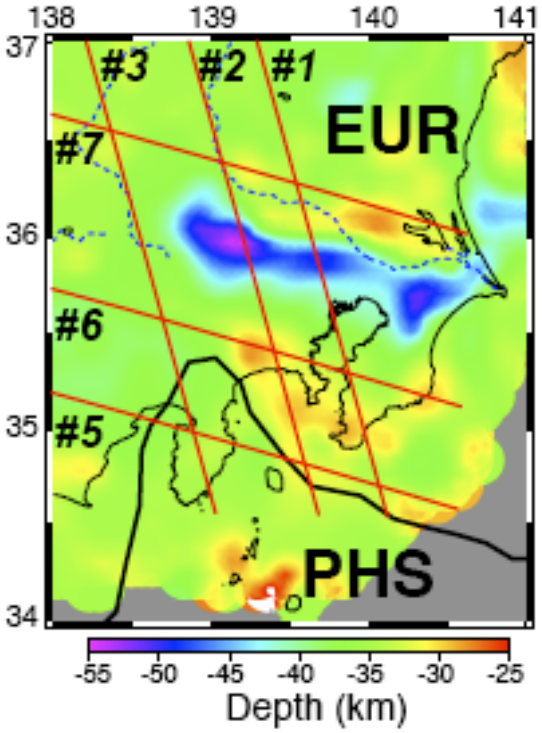

Figure 5. Depth to iso-velocity surface of 7.5 km/sec. Depth scale in km. The blue area corresponds to a trough down to about 55 km. Position of deep trough represents location of tectonic erosion of EUR crust to north and thus indicates the spatial positioning of the top-of-PHS.

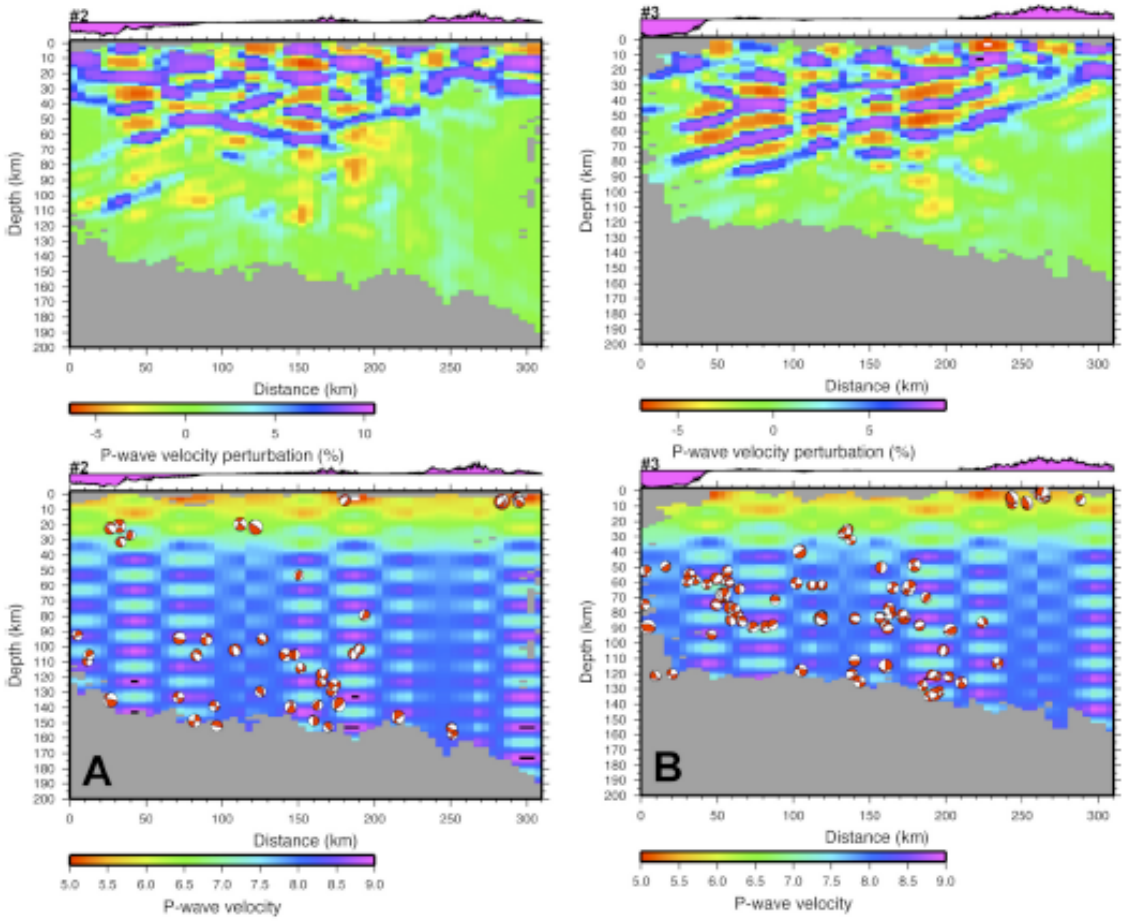

Figure 6. Checkerboard resolution test for two nearly N-S profiles in Fig. 3 (A) for profile #2 and (B) for profile #3 . The bottom profile in each figure shows the synthetic model and the top file shows the recovered anomalies.

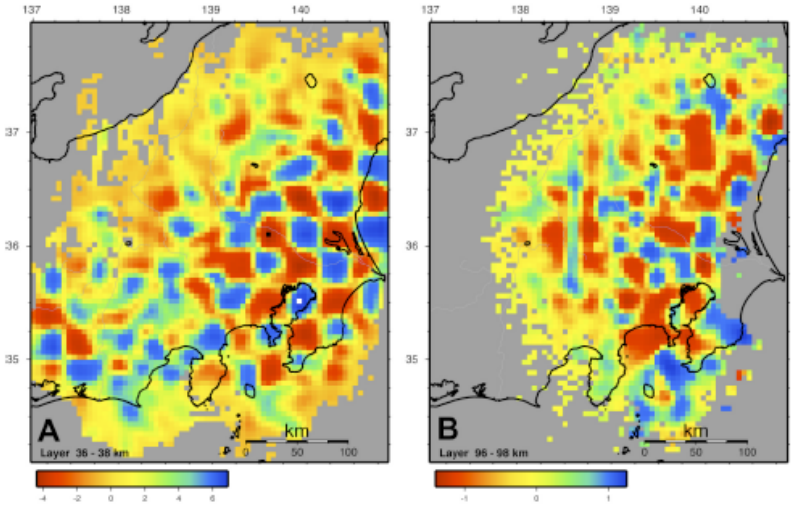

Figure 7. Checkerboard resolution plotted at two depths: (a) at 16-18 km depth
and (b) at 96-98 km level.